Plant water use responses along secondary forest succession during the 2015–2016 El Niño drought in Panama

Mario Bretfeld[1,2] (iD), Brent E. Ewers[3] and Jefferson S. Hall[1]

[1]ForestGEO, Smithsonian Tropical Research Institute, Av. Roosevelt 401, Balboa, Ancón, Panama; [2]Department of Botany, University of Wyoming, Laramie, WY 82071, USA; [3]Department of Botany and Program in Ecology, University of Wyoming, Laramie, WY 82071, USA

Author for correspondence:
Mario Bretfeld
Tel: +1 307 343 3737
Email: m.bretfeld@gmail.com

Summary

- Tropical forests are increasingly being subjected to hotter, drier conditions as a result of global climate change. The effects of drought on forests along successional gradients remain poorly understood.
- We took advantage of the 2015–2016 El Niño event to test for differences in drought response along a successional gradient by measuring the sap flow in 76 trees, representing 42 different species, in 8-, 25- and 80-yr-old secondary forests in the 15-km² 'Agua Salud Project' study area, located in central Panama.
- Average sap velocities and sapwood-specific hydraulic conductivities were highest in the youngest forest. During the dry season drought, sap velocities increased significantly in the 80-yr-old forest as a result of higher evaporative demand, but not in younger forests. The main drivers of transpiration shifted from radiation to vapor pressure deficit with progressing forest succession. Soil volumetric water content was a limiting factor only in the youngest forest during the dry season, probably as a result of less root exploration in the soil.
- Trees in early-successional forests displayed stronger signs of regulatory responses to the 2015–2016 El Niño drought, and the limiting physiological processes for transpiration shifted from operating at the plant–soil interface to the plant–atmosphere interface with progressing forest succession.

Introduction

Ecosystems world-wide are being subjected to increasing pressure from climate change, and plant water use traits are a crucial component towards the development of a predictive understanding of plant responses to these changes. Globally, 2015 marked the warmest year since the beginning of instrumental data collection with temperature anomalies exceeding two standard deviations (2SD) in the tropics (Hansen & Sato, 2016). Tropical forests are particularly sensitive to drought and respond with considerable changes in species distribution and composition (Engelbrecht *et al.*, 2007; Nepstad *et al.*, 2007; Phillips *et al.*, 2009; Wright, 2010). The 2015–2016 El Niño-Southern Oscillation (ENSO) event provided an excellent research opportunity to study the responses of tropical forests to severe drought conditions. In Panama, the 2015–2016 ENSO event resulted in the third longest dry season on record (173 d) with over 90% of the country experiencing severe drought conditions. A mechanistic understanding of the responses to drought of tropical forests is critical to land management and conservation efforts, and to the improvement of the predictive power of global models of carbon and water fluxes that generally perform poorly under drought conditions (Powell *et al.*, 2013).

Hydraulic failure is a main driver of drought-induced tree mortality in tropical forests (Rowland *et al.*, 2015). However,

studies assessing the drought responses of tropical trees across a successional gradient are often based on seedlings/saplings or monospecific stands (e.g. Huc *et al.*, 1994; Tyree *et al.*, 2003; Engelbrecht *et al.*, 2006; Markesteijn *et al.*, 2011; Pineda-Garcia *et al.*, 2012, 2015), and field data are sparse. As a result of the high taxonomic diversity and lack of species dominance in most tropical forests, a trait-based approach to data analysis (McGill *et al.*, 2006; Escudero & Valladares, 2016) is often the only cost-effective way to study these forests. For example, leaf and stem hydraulic traits explained drought tolerance across species in Amazon rainforest trees (Powell *et al.*, 2017), and similar morphological characteristics (e.g. sapwood depth, tree size, phenology) appear to outweigh taxonomic affiliation, as indicated by considerable convergence in sap flow among phylogenetically diverse, but morphologically similar, species in tropical systems (Meinzer *et al.*, 2001; O'Brien *et al.*, 2004; McJannet *et al.*, 2007; Kunert *et al.*, 2010; Moore *et al.*, 2017). Recent work on sap flow in subtropical and tropical biomes includes the assessment of responses to drought (Luo *et al.*, 2016), environmental factors (Eller *et al.*, 2015; Aparecido *et al.*, 2016) and seasonal variability (Kunert *et al.*, 2010; Schwendenmann *et al.*, 2015).

Early-successional, light-demanding species are generally characterized by lower wood density, larger vessel diameter and specific leaf area, coinciding with higher hydraulic conductivity and

sap velocities compared with late-successional species (Bazzaz & Pickett, 1980; Poorter *et al.*, 2004, 2010; Markesteijn *et al.*, 2011; Apgaua *et al.*, 2015; Schönbeck *et al.*, 2015). Although these traits suggest that early-successional species are more vulnerable to xylem cavitation (Tyree & Sperry, 1989), some studies have reported no difference (Pineda-Garcia *et al.*, 2012, 2015; Powell *et al.*, 2017) or lower drought tolerance in late-successional species (Apgaua *et al.*, 2015; Schönbeck *et al.*, 2015). Independent of their successional classification, larger trees have the potential to mitigate drought effects through stem capacitance and access to deep soil water (Phillips *et al.*, 2003; Čermák *et al.*, 2007; Schwendenmann *et al.*, 2015).

Recent studies have suggested that drought-induced mortality is most common at the end of the growth spectrum, with highest mortalities reported at the seedling stage and in large trees (Engelbrecht *et al.*, 2006; Nepstad *et al.*, 2007; Rowland *et al.*, 2015; Meakem *et al.*, 2017). In the moist lowland forests of Panama, transpiration in canopy trees is generally energy limited as a result of frequent cloud cover and abundant soil water content, especially during the rainy season (Graham *et al.*, 2003), and regulated by structural (leaf area) rather than physiological (stomatal control) means (Phillips *et al.*, 2001; Wolfe *et al.*, 2016). An understanding of both plant hydraulic conductivity and response to environmental drivers is crucial to improve the predictive understanding of drought responses. When soil water and plant water transport are non-limiting, transpiration is a function of the available energy (radiation) and atmospheric dryness (vapor pressure deficit, VPD), that is, atmospheric demand (Penman, 1948; Monteith, 1965). Diel transpiration is approximately linearly related to radiation or VPD – whichever is more limiting – until maximum hydraulic conductivity occurs and saturation of transpiration is reached (Oren *et al.*, 1999). Thus, deviations from these linear relationships can be indicative of regulatory responses, such as stomatal closure or hydraulic limitations, and statistical modeling of these deviations can be used to detect parameters that limit transpiration, such as soil volumetric water content (VWC) (Oren *et al.*, 1998; Eller *et al.*, 2015). Moreover, time lags and hysteresis patterns in the diurnal relationship between transpiration, VPD and photosynthetic photon flux density (PPFD) can be used to determine the biotic and abiotic factors that limit transpiration (O'Grady *et al.*, 1999; Phillips *et al.*, 1999; Matheny *et al.*, 2014; Zhang *et al.*, 2014; Mallick *et al.*, 2016). In addition, nocturnal sap flow can be an indicator of stem refilling of capacitance storage in drought-stressed trees (Pfautsch & Adams, 2013) and has been shown to be significantly higher in dry season than wet season periods in tropical biomes (Forster, 2014).

The main objective of this study was to elucidate the interactions between plant hydraulics, successional stage and environmental drivers in species-diverse secondary tropical forests during the severe drought of the 2015–2016 ENSO event in central Panama. Utilizing a chronosequence approach, we measured sap flow in 8-, 25- and 80-yr-old secondary forests and tested the following hypotheses. Early-successional forests exhibit highest overall sap velocities and sapwood-specific hydraulic conductivities as a result of typically higher leaf area allocation and leaf-level water

demand of fast-growing, shade-intolerant pioneer species. Early-successional forests experience reduced sap velocities during the dry season drought as a result of presumed shallower rooting depth in 8-yr-old trees relative to 80-yr-old trees, and exhibit strong regulatory responses and opportunistic water use strategies. Late-successional forests exhibit no decrease in sap velocities during drought periods as a result of presumed access to deep soil water reservoirs and stem water storage in larger trees. Sap velocities in early-successional forests are mainly driven by radiation as a result of high exposure in a single-layered forest and the prevalence of opportunistic pioneer species, whereas VPD is the main driver of sap velocities in late-successional forests as a result of the presence of a multi-layered, partially shaded canopy with a higher proportion of shade-adapted species.

Materials and Methods

Study area

All sites were located in the 'Agua Salud Project' study area (AS), located centrally in the Panama Canal Watershed (PCW; 9°13′N, 79°47′W, 330 m above sea level, asl). The study area borders Soberania National Park to the west and comprises a mosaic of land use types that are typical for the PCW, including cattle pastures, fallows, timber plantations and secondary forest patches. Local topography is characterized by rolling hills with steep slopes and a dense network of small streams. Soils are deep Oxisols with relatively low fertility (Turner & Engelbrecht, 2011). The climate is sub-humid tropical, with an annual mean precipitation of 2700 mm and a pronounced dry season from late December to mid-May (Ogden *et al.*, 2013). In 2015, strong ENSO conditions resulted in only 1800 mm of precipitation, and 2014–2016 marked the driest contiguous 3-yr period since the beginning of instrumental data collection in 1925 on Barro Colorado Island, located *c.* 12 km southwest from the study area (data provided by the Physical Monitoring Program of the Smithsonian Tropical Research Institute).

We used a chronosequence approach to monitor transpiration across a successional gradient in secondary forests throughout the 2015–2016 ENSO event. Despite the known limitations of chronosequence studies (Johnson & Miyanishi, 2008) and the reported uncertainties of successional trajectories in neotropical forest successions (Norden *et al.*, 2015), there is sufficient support for this approach in the literature. In the AS project area, early-successional forests are more similar to one another than are late-successional forests, both with regard to composition (van Breugel *et al.*, 2013) and functional traits (Craven *et al.*, 2015). In addition, general trends in biophysical traits are largely independent of taxonomic affiliation and a tight link exists between these traits and water use strategies (Ewers *et al.*, 2011). We studied three stands of secondary forest, including young (hereafter SF8 for secondary forest of 8 yr of age at the beginning of data collection), 25-yr-old and 80-yr-old forest (hereafter SF25 and SF80). All three stands were utilized as cattle pasture before stand initiation; the basal areas were 9.4, 16.0 and 31.5 m^2 ha^{-1} for SF8, SF25 and SF80, respectively (Supporting information

Table S1; van Breugel *et al.*, 2013). Sap flow was measured on one hillslope each in SF8 and SF80, and two hillslopes in SF25, at the halfway point between ridgetop and valley bottom, with total slope distances of 139, 103/104 and 60 m in SF8, SF25 and SF80, respectively. Slopes were 29°, 29°/33° and 24° and aspects were 219°, 242°/70° and 202° in SF8, SF25 and SF80, respectively. Elevations at the center of each sap flow site were 264, 276/246 and 190 m asl in SF8, SF25 and SF80, respectively.

Sap flow measurements

We used heat ratio sap flow sensors (Marshall, 1958) to measure sap flow in 76 trees, representing 46 species, across all sites (Table S2). Initial tree selection was based on diameter at breast height (DBH) to represent local size distribution rather than species. In a landscape-scale study of forest succession in the AS project area, van Breugel *et al.* (2013) found that only six of the 526 plant species made up > 5% of all plants ≥ 1 cm in diameter in > 10% of their 108 plots. Thus, most locally dominant species were not dominant across the metacommunity and the selection of species on the basis of local dominants can result in biased samples. We included small and understory trees to ensure adequate representation of establishing late-successional trees to capture a wider range of canopy positions, especially in older forests. Based on relative canopy position, 13 of the 27 instrumented trees in SF80 were classified as sub-canopy trees, compared with three and zero sub-canopy trees in SF25 and SF8, respectively. Lastly, tree size has been shown to be more important than species affiliation when determining sap velocities in a multispecies forest (Hernandez-Santana *et al.*, 2015; Moore *et al.*, 2017). All selected trees were identified to species level and compared with their local abundance based on basal area data from nearby secondary succession plots (van Breugel *et al.*, 2013). Based on these data, we identified two species in SF8 (*Conostegia xalapensis*, *Vismia macrophylla*) and two species in SF25 (*Xylopia frutescens*, *V. macrophylla*) which each accounted for at least 5% of basal area in all four and all three nearby secondary succession plots in SF8 and SF25, respectively. As a result, two additional individuals of *C. xalapensis* and one individual of *V. macrophylla* were instrumented in SF8 to better represent these locally (pre-)dominant species, whereas *X. frutescens* and *V. macrophylla* were already adequately represented in SF25 with five and four instrumented trees, respectively (Table S2). No dominant species were identified in SF80.

Sensors were installed at breast height (*c.* 1.37 m) on the upslope-facing side of the tree and were placed equidistant from the heater using a drill guide. Despite potential radial variation in sap flow, we used one sensor per tree rather than multiple sensors per tree. Given a limited number of sensors, this approach has been shown to reduce uncertainties in estimates of stand-scale sap flow measurements (Komatsu *et al.*, 2017). Sensors were constructed using stainless steel hypodermic needles (1.3 mm in diameter) cut to either 26 or 13 mm in length. A copper-constantan thermocouple junction was inserted into the needle with effective measurement depths of 20 mm (for use in trees with DBH > 5 cm) and 10 mm (for use in trees with DBH < 5 cm) for 26- and 13-mm needles, respectively. Heaters were constructed using slightly larger needles (1.6 mm in diameter) to accommodate constantan coils. All needles were sealed with epoxy at the tip and with hot glue at the fitting. To account for expectedly high flow rates, we chose a sensor spacing of 0.5 cm (Burgess *et al.*, 2001).

Data were logged in 30-min intervals following a 3-s heat pulse and downloaded weekly beginning in 2015 on 12 March (SF25), 21 May (SF8) and 29 July (SF80) until 31 August 2016 (Table S3). To minimize noise and to allow for the equilibration of temperature ratios (Burgess *et al.*, 2001), 20 measurements were logged and averaged after a 60-s delay following the pulse of heat. At each site, sensors were connected via differential channels to two AM16/32 multiplexers (Campbell Scientific, Logan, UT, USA), controlled by a single CR1000 data logger (Campbell Scientific). Measured temperature ratios were converted to heat pulse velocities V_h (cm h^{-1}) according to Burgess *et al.* (2001):

$$V_h = \frac{k}{x} \ln\left(\frac{v_1}{v_2}\right) 3600 \qquad \text{Eqn 1}$$

where k is the thermal diffusivity of wood (cm^2 s^{-1}), x is the distance between heater and either sensor (cm) and v_1/v_2 is the temperature ratio between downstream and upstream sensors. V_h was corrected for wounding according to the numerical solution by Burgess *et al.* (2001) and converted to sap velocity V_s (cm h^{-1}; Marshall, 1958; Barrett *et al.*, 1995):

$$V_s = \frac{V_c \rho_b (c_w + m_c c_s)}{\rho_s c_s} \qquad \text{Eqn 2}$$

where ρ_b is the wood density (g cm^{-3}), c_w and c_s are specific heat capacities of wood and water (J kg^{-1} K^{-1}), respectively, m_c is the water content of sapwood and ρ_s is the density of water (g cm^{-3}). Wood properties of instrumented tree species were taken from a local dataset (Wright *et al.*, 2010). To account for potential probe misalignment, we induced zero-flow conditions by severing xylem vessels using a battery-powered oscillating saw (DeWalt, model DCS355D1; Towson, MD, USA). Incisions were 4 cm wide, 6 cm deep and located 3 cm above and below the sensors on a subset of trees with sufficiently large diameters to reduce the risk of wound-induced mortality. After validation of zero flow, a new set of sensors was installed on the same tree. Zero-flow conditions were also assumed to occur predawn (03:00–04:30 h) during periods with low atmospheric demand for water (VPD < 0.2 kPa). Data from induced zero-flow measurements were used to validate data from assumed zero-flow conditions. Of the 76 instrumented individuals, data from six individuals were excluded from the analysis as a result of mortality (four trees) and high noise levels in the data (two trees; Table S2). No gap filling was performed.

Micrometeorological measurements

A meteorological station within the AS project area provided local climate data, including net radiation (W m^{-2}) using a CN4 net radiometer (Kipp & Zonen, Delft, the Netherlands), air

temperature (°C) and relative humidity (RH, %) using an HMP60 (Vaisala, Vantaa, Finland), PPFD (μmol m^{-2} s^{-1}) using a PSQ1 quantum sensor (Kipp & Zonen), precipitation (mm) using a 260-250-A tipping bucket (NovaLynx, Grass Valley, CA, USA) and wind speed (WS, m s^{-1}) using a 05103 wind anemometer (R. M. Young, Traverse City, MI, USA). VPD (kPa) was calculated from these data following Allen *et al.* (1998). In each forest, soil VWC was measured in three locations along the hillslope using GS1 sensors (Decagon Devices, Pullman, WA, USA) at three measurement depths (10, 30 and 50 cm) each. A single term for VWC was calculated, based on the weighted-by-depth average of data from 10, 30 and 50 cm depths.

Hydraulic conductivity

Leaf water potentials Ψ_L were measured in the dry (6–16 March 2016) and wet (26–28 July 2016) seasons using a pressure chamber (PMS Instrument Company, Albany, OR, USA). In all forests, data were collected at predawn (03:00–05:00 h), midday (11:00–14:00 h) and predusk (17:00–19:00 h). Data collection was limited to instrumented trees whose canopy could be clearly distinguished from that of neighboring trees and that could be reached using 5-m-long pole pruners ($N_{SF8} = 7$, $N_{SF25} = 8$, $N_{SF80} = 11$). To test for within-tree heterogeneity of Ψ_L, we sampled 36 leaves from different positions within the canopy (lower canopy sun, lower canopy shade, upper canopy sun, upper canopy shade) from nine trees representing eight species in SF80 using a sling shot at midday (11:00–13:00 h) during the dry season on 22 February 2017, when Ψ_L gradients in the canopy are likely to be most pronounced. Lower canopy leaves were sampled between 2 and 5 m in height, and upper canopy leaves were sampled between 15 and 25 m in height. ANOVA results showed no significant difference in Ψ_L at different canopy positions ($P = 0.57$, Fig. S1), suggesting that lower canopy samples can be used as a proxy for average Ψ_L throughout the canopy. Similarly small gradients in Ψ_L have been found by Oberbauer *et al.* (1987) in Costa Rica.

Darcy's law-approximated sapwood-specific conductivity K_s was calculated for each tree (Tyree & Ewers, 1991) from the slope parameter of simple linear regression of sap flux density and leaf water potentials (Martínez-Vilalta *et al.*, 2014). Several assumptions are associated with this approach. First, we assumed homogeneous sap flow throughout the sapwood and accordingly calculated the volume of sap flowing across an area of sapwood based on the conversion of V_s (cm h^{-1}) to sap flux density J (cm^3 m^{-1} s^{-1}). Second, we assumed that Ψ_L measurements are representative of average canopy Ψ_L (see previous paragraph). Third, the approach accounts for the assumptions of obtaining Ψ_L at true peak sap flow and uncertainties of equilibration of soil water potential Ψ_S and Ψ_L at predawn (Martínez-Vilalta *et al.*, 2014; Hochberg *et al.*, 2017). Lastly, to account for vertical heterogeneity in V_s (i.e. stem hydraulic capacitance), we used sap flow data at the timestamp with the highest correlation coefficient between evaporative demand and up to 90-min time-lagged sap flow rates on the day of water potential measurements for each

tree. Evaporative demand (m s^{-1}) was calculated according to Van Bavel (1966) and Bladon *et al.* (2006).

$$\text{ET}_p = \frac{\Delta Q^* + \rho_a c_a u D}{\rho_\omega \lambda_\upsilon (\Delta + \gamma)} \qquad \text{Eqn 3}$$

where Δ is the slope of the saturation vapor pressure curve (Pa K^{-1}), Q^* is the net radiation (J m^{-2} s^{-1}), ρ_a is the density of air (kg m^{-3}), c_a is the heat capacity of air (J kg^{-1} K^{-1}), u is WS (m s^{-1}), D is VPD (Pa), ρ_ω is the density of water (kg m^{-1}), λ_υ is the latent heat of vaporization (J kg^{-1}) and γ is the psychrometric constant (Pa K^{-1}). A total of 203 measurements were included in the analysis and the resulting K_s values were averaged by forest age.

Statistical analysis

As a result of the robustness of linear mixed models in dealing with longitudinal data with missing data as well as temporal autocorrelation (von Ende, 2001), a linear mixed model (M-1) was used to assess differences in average seasonal V_s or K_s (response) between seasons, forest age and the interaction between season and forest age (fixed effects), whilst accounting for individual trees (random effect). Seasons were classified according to official dates provided by the Meteorological and Hydrological Branch of the Panama Canal Authority, with the wet seasons starting on 17 May (2015) and 27 April (2016), and the dry seasons starting on 27 November (2015) and 19 December (2016). Analysis was limited to a subset of trees for which data were available in all seasons ($N_{SF8} = 15$, $N_{SF25} = 25$, $N_{SF80} = 26$). Differences in V_s and K_s between seasons for a given forest age were assessed via least square means pairwise comparisons. One-sample t-tests were used to test whether nocturnal flow was significantly different from zero for each forest and season. Where multiple tests were performed, the Bonferroni correction was applied to account for multiple comparisons. A second linear measure mixed model (M-2) was used to assess differences in the effects of VPD, PPFD, WS, precipitation and VWC on average daily V_s between forest ages, accounting for random effects of seasons and individual trees. Despite the known interaction between VPD and PPFD (i.e. evaporative demand; Eqn 3) and their separate mechanistic impacts on transpiration (Bladon *et al.*, 2006), we chose to separate these parameters to be able to test for potential differences caused by successional shifts in shade tolerance and canopy structure. Model parameters were statistically evaluated using the Markov chain Monte Carlo method with 1000 iterations (R-package 'MCMCGLMM'; Hadfield, 2010). For comparative analyses between forest ages using models M-1 and M-2, data were limited to 29 July 2015 to 31 August 2016 when data were collected in all forests. Wood densities were assessed for differences between forests via ANOVA. Differences in Ψ_L and soil VWC between forests were assessed by linear mixed models and least square means pairwise comparisons. Mixed effect model analyses were performed using the R-package 'LME4' (Bates *et al.*, 2015) and pairwise comparisons using the R-package 'MULTCOMP' (Hothorn *et al.*, 2008).

A linear regression model was developed with VPD, PPFD, WS, precipitation and VWC as predictors and average daily V_s across trees per forest age as response. To minimize within-forest variance, the relationship between the standard deviation of daily mean V_s and sample size was assessed (Fig. S2). Subsequently, only days with data from at least 10 (SF8 and SF25) or 15 (SF80) trees were included in the analysis. Linear regression models were based on Box–Cox transformed data beginning from the earliest time of measurement in each forest (Box & Cox, 1964). Relative importance metrics of environmental predictors were calculated (R-package 'RELAIMPO'; Grömping, 2006), including each predictor's usefulness (model contribution given all other predictors already included in the model) and overall model contribution averaged over orderings of predictors (Chevan & Sutherland, 1991). To account for a potential size effect, we performed a separate analysis of relative importance metrics on a subset of trees smaller than 15 cm DBH in SF25 and SF80. Confidence intervals for relative importance metrics were calculated via bootstrapping (1000 runs). All data processing and analyses were performed in R 3.3.2 (R Core Team, 2015).

Results

Diel patterns of V_s closely followed VPD and PPFD in all forests, with V_s lagging slightly behind PPFD in SF8 and SF80, but not in SF25 (Fig. 1). In all forests, a clockwise hysteresis was evident between normalized half-hourly V_s and VPD, especially during the dry season, and a counter-clockwise hysteresis was evident in the relationship between V_s and PPFD, especially in SF8 and SF80 (Fig. 2). Average Ψ_L during the dry season was similar among forests, ranging from -0.4 to -0.6 and from -1.6 to -1.7 MPa at predawn and midday, respectively (Fig. 3a). Predusk Ψ_L was significantly less negative in SF8 than SF80 ($P = 0.04$), with -0.9 and -1.4 MPa, respectively. In the wet season, average Ψ_L was similar among all forests, ranging from -0.3 to -0.4 and from -0.4 to -0.5 MPa at predawn and
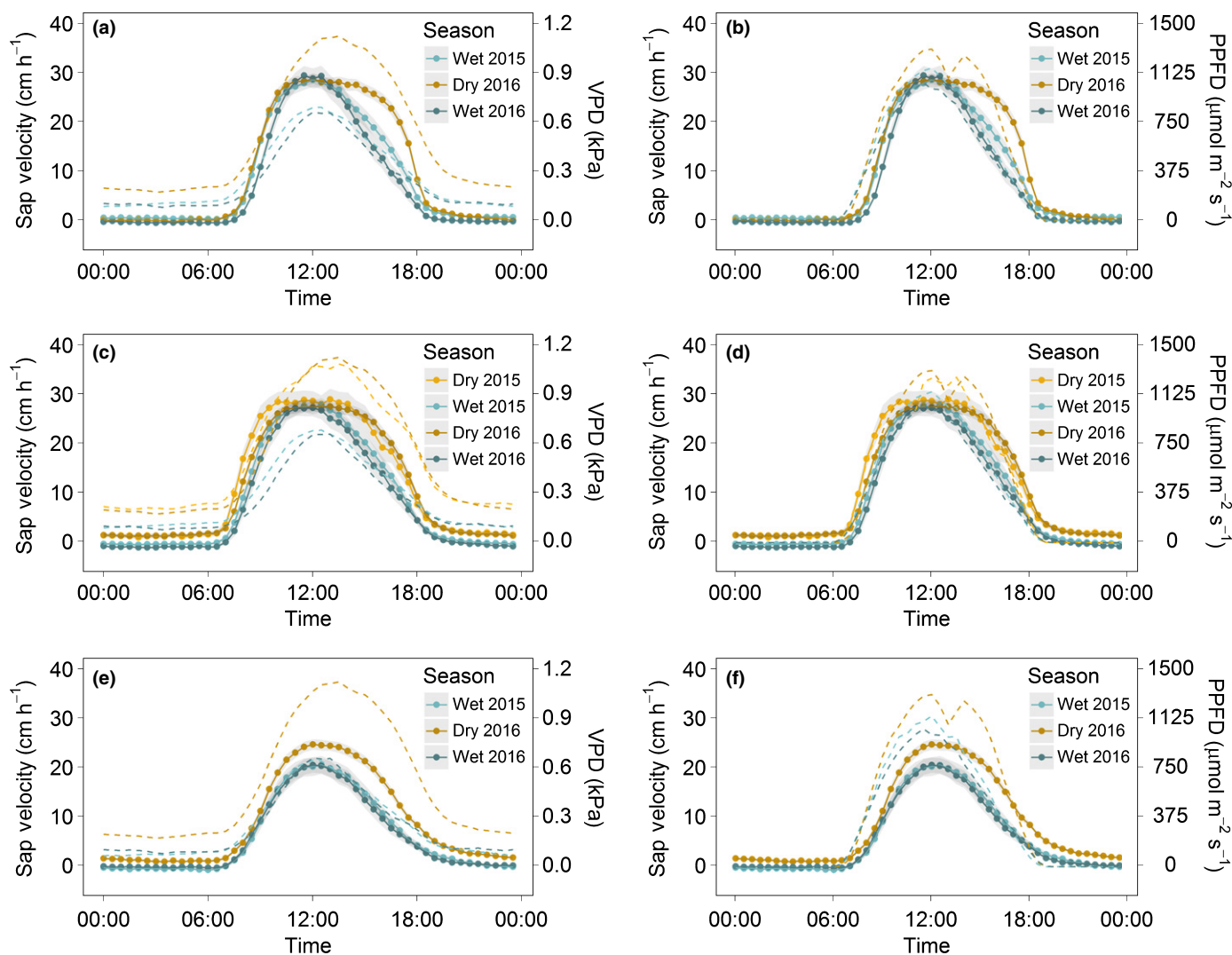

Fig. 1 Diel patterns of sap velocity (cm h^{-1}) based on half-hourly averages from all trees in (a, b) SF8, (c, d) SF25 and (e, f) SF80. Shaded areas represent 95% confidence intervals. The dashed lines indicate half-hourly averages of (a, c, e) vapor pressure deficit (VPD in kPa) and (b, d, f) photosynthetic photon flux density (PPFD in μmol m^{-2} s^{-1}).
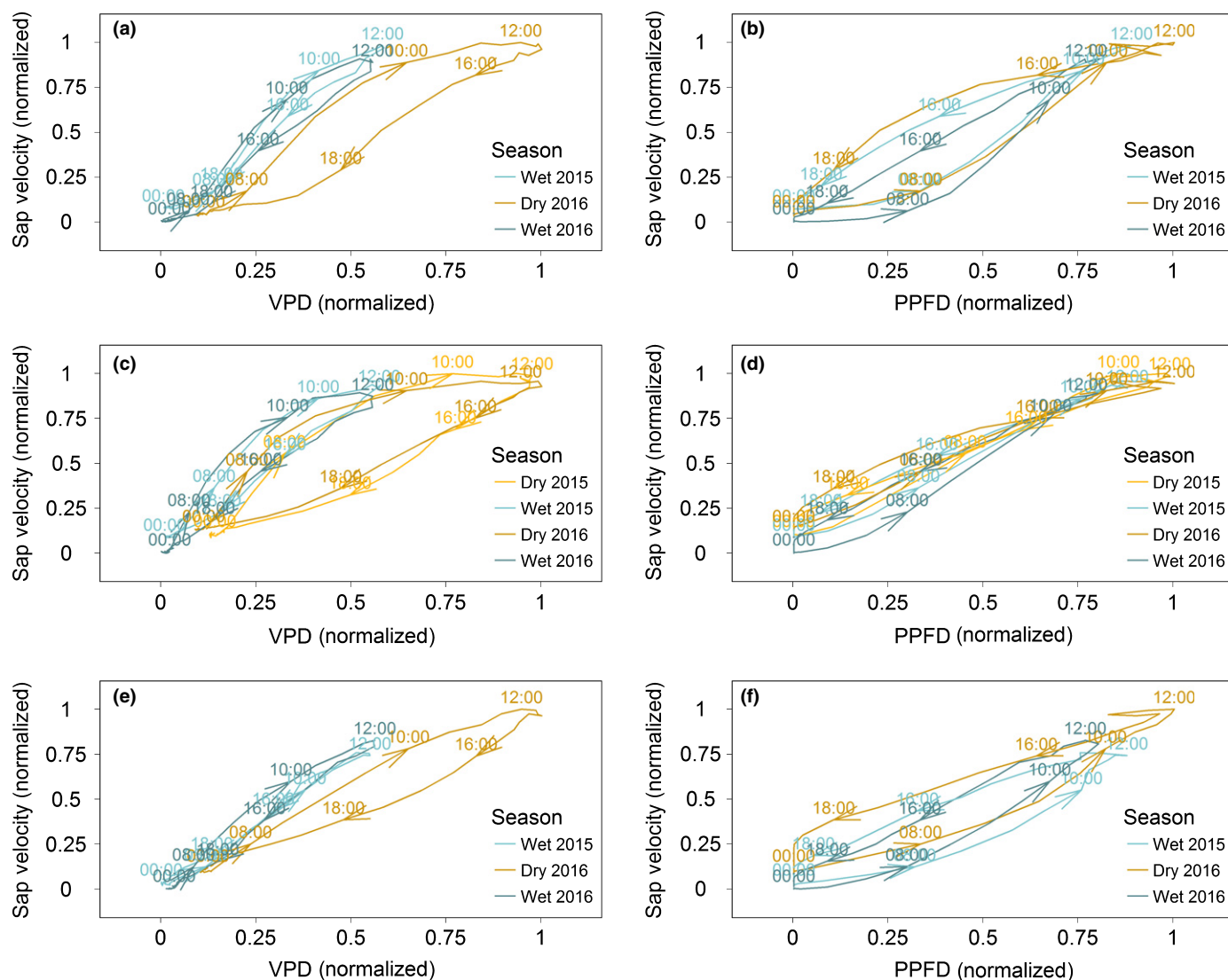
Fig. 2 Hysteresis loops between (a, c, e) normalized sap velocities and normalized vapor pressure deficit (VPD), and (b, d, f) normalized sap velocities and normalized photosynthetic photon flux density (PPFD) in (a, b) SF8, (c, d) SF25 and (e, f) SF80. Arrows indicate direction of hysteresis.

predusk, respectively (Fig. 3b). Midday Ψ_L was significantly less negative in SF80 than in SF8 ($P < 0.001$) and SF25 ($P = 0.018$), with -0.4, -0.7 and -0.9 MPa, respectively. Significant night-time sap flow occurred during the dry season in SF25 (2.01 cm h^{-1}; $P = 0.002$) and SF80 (1.90 cm h^{-1}; $P < 0.001$), reaching 11% and 8.7% of average daytime V_s in SF25 and SF80, respectively (Table 1). Night-time flow was not significant in SF8 or during wet season periods in any forest.

Seasonality had a significant effect on V_s, as reflected in clear seasonal patterns across all forests (M-1, $P < 0.001$; Table 2; Fig. 4). Although average V_s tended to be highest in SF8 and decreased with increasing forest age, the differences among forests were nonsignificant (Table 2; Fig. 5). In SF80, average V_s was significantly higher in the dry season compared with both wet seasons ($P < 0.01$), whereas no significant differences between seasons were detected in SF8 and SF25 (Table 2). Seasonality also had a significant effect on K_s ($P = 0.013$). In July 2016 (wet season), K_s values were 5.81 ± 2.14, 5.22 ± 2.2 and 1.75 ± 1.3 mol m^{-2} s^{-1} MPa^{-1}

in SF8, SF25 and SF80, respectively (Fig. 6). Compared with wet season values, K_s in the dry season (March 2016) decreased significantly by 69% ($P = 0.013$) and 75% ($P < 0.001$) to 1.8 ± 1.17 and 1.3 ± 0.42 mol m^{-2} s^{-1} MPa^{-1} in SF8 and SF25, respectively. In SF80, the wet to dry season increase of K_s by 5% to 1.84 ± 0.44 mol m^{-2} s^{-1} MPa^{-1} was not significant. Wood densities were not significantly different between forests ($P = 0.06$), with mean and standard error (SE) values of 0.59 ± 0.02, 0.53 ± 0.02 and 0.59 ± 0.02 g cm^{-3} in SF8, SF25 and SF80, respectively.

When accounting for seasonal and daily variance (M-2), significant differences in age-specific behavior and responses to environmental variables were detected. All environmental main effects (VPD, PPFD, WS, precipitation, VWC) and the interactions between forest age and VPD, PPFD, WS and VWC were significant (Table S4). Model parameter estimates suggested that VPD was a strong driver of V_s in all forests, with slopes of 3.81, 4.74 and 5.58 in SF8, SF25 and SF80, respectively. Precipitation
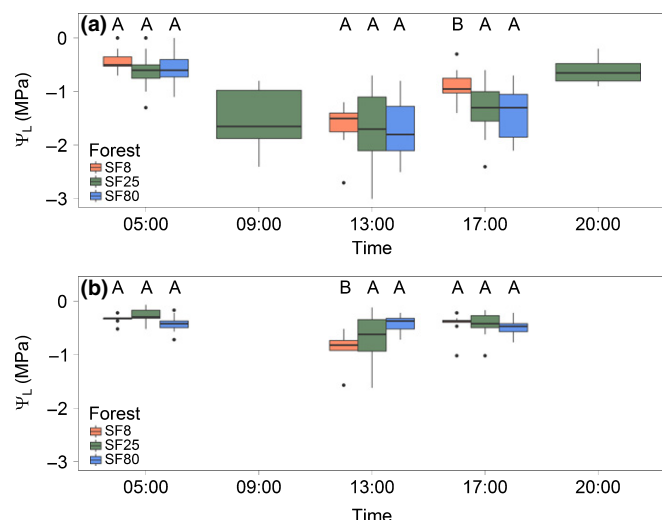
Fig. 3 Leaf water potentials Ψ_L in MPa in (a) the dry season (6–16 March 2016) and (b) the wet season (26–28 July 2016) for SF8 (orange), SF25 (green) and SF80 (blue). Horizontal lines inside boxes correspond to the median, the lower and upper box boundaries correspond to the first and third quartiles (25th and 75th percentiles, respectively), lower and upper whiskers extend no further than 1.5× inner quartile range (IQR) from the first and third quartiles, and dots represent data points beyond this range. Letters indicate significant differences in average leaf water potential between forests at a given sampling time as assessed via linear mixed model and least square means pairwise comparison. Data from 09:00 and 20:00 h were only collected in SF25 in the dry season.

Table 1 Summary statistics and *t*-test results (Bonferroni-adjusted alpha for nine tests: 0.0056) for average nocturnal sap velocities by seasons and forest age

Forest	Season	n	Nocturnal V_s (cm h^{-1})	SE	95% confidence interval	P value
SF8	Wet 2015	15	0.86	0.52	1.12	0.12
	Dry 2016	15	0.51	0.56	1.20	0.37
	Wet 2016	15	−0.26	0.67	1.44	0.71
SF25	Wet 2015	25	−0.61	0.64	1.32	0.35
	Dry 2016	25	2.01	0.57	1.78	0.002*
	Wet 2016	25	−0.48	0.53	1.09	0.37
SF80	Wet 2015	26	0.18	0.44	0.91	0.69
	Dry 2016	26	1.90	0.39	0.79	<0.001*
	Wet 2016	26	0.16	0.35	0.72	0.65

All analyses based on trees for which data were collected in all seasons ($N_{SF8} = 15$, $N_{SF25} = 25$, $N_{SF80} = 26$). Data from 29 July 2015 to 31 August 2016. *, $P < 0.05$.

was the only main effect with a negative slope parameter (−0.05). The effect of VPD on V_s was significantly greater in SF80 than in SF8, and the effect of PPFD was significantly greater in both SF8 and SF25 compared with SF80. WS had a significantly greater effect on V_s in SF25 compared with both SF8 and SF80. Soil VWC parameter estimates were significantly different between all forests and were the only model parameters with changing signs, with positive slopes for SF8 (0.2) and SF25 (0.08) and a negative slope for SF80 (−0.11).

Table 2 ANOVA table of generalized linear mixed model results of average sap velocities per season (M-1) and least square means pairwise comparison for average diel sap velocities between seasons by forest age (Tukey's single step)

	Sum of squares	Mean square	df	F value	P value
Forest age	26.26	13.13	2	1.28	0.28
Season	156.78	78.39	2	7.65	<0.001*
Forest age : season	45.36	11.34	4	1.11	0.36

Forest	Contrast	Estimate	SE	t value	P value
SF8	Wet 2015 – Dry 2016	−0.54	1.17	−0.46	0.89
	Wet 2015 – Wet 2016	1.40	1.17	1.19	0.46
	Dry 2016 – Wet 2016	1.94	1.17	1.66	0.22
SF25	Wet 2015 – Dry 2016	−1.55	0.91	−1.72	0.20
	Wet 2015 – Wet 2016	−0.28	0.91	−0.31	0.95
	Dry 2016 – Wet 2016	1.28	0.91	1.41	0.34
SF80	Wet 2015 – Dry 2016	−3.02	0.89	−3.40	0.003*
	Wet 2015 – Wet 2016	0.13	0.89	0.15	0.99
	Dry 2016 – Wet 2016	3.15	0.89	3.55	0.002*

Analyses based on trees for which data were collected in all seasons ($N_{SF8} = 15$, $N_{SF25} = 25$, $N_{SF80} = 26$). Data from 29 July 2015 to 31 August 2016. *, $P < 0.05$.

Single-variable linear regression of VPD and V_s explained 48%, 54% and 71% in SF8, SF25 and SF80, respectively (Fig. 7a,c, e). In SF8 and SF25, residuals showed a distinct pattern when plotted against VWC below 40% (Fig. 7b,d,f). Below this threshold, VWC explained 42% ($P < 0.001$) and 7% ($P < 0.001$) of the residuals in SF8 and SF25, respectively, whereas no significant relationship between residuals and VWC was detected in SF80. Single-variable regression of PPFD and V_s explained 60%, 59% and 66% in SF8, SF25 and SF80, respectively, with similar relationships between residuals and VWC as above (Fig. S3). The proportions of variance explained by linear regression including all predictors were 69%, 66% and 86% in SF8, SF25 and SF80, respectively. Overall model contributions averaged over orderings of predictors showed that PPFD and VPD were the main drivers of V_s, together accounting for 77%, 71% and 63% of model strength in SF8, SF25 and SF80, respectively (Table 3). With progressing forest age, VPD replaced PPFD as the primary driver of V_s. The parameter usefulness of WS increased with increasing forest age from 3% in SF8, to 12% and 13% in SF25 and SF80, respectively, whereas the parameter usefulness of VWC decreased from 31% in SF8 to 11% and 4% in SF25 and SF80, respectively (Table 3).

Of the species that were classified as deciduous or semi-deciduous (Table S2), most exhibited only brief periods of dormancy at varying times throughout the year. However, the simultaneous, prolonged dormancy of four *Annona spraguei* and one *Casearia arborea* caused a sharp decline in average V_s in SF25 at the dry–wet transition in April 2016 (Fig. 4). Excluding the aforementioned trees from the analysis resulted in a less dramatic drop and overall higher V_s at the end of the dry season in SF25 (Fig. S4), improved linear regression model performance in SF25 to 72% and reduced parameter usefulness of VWC to 2% (Table S6).
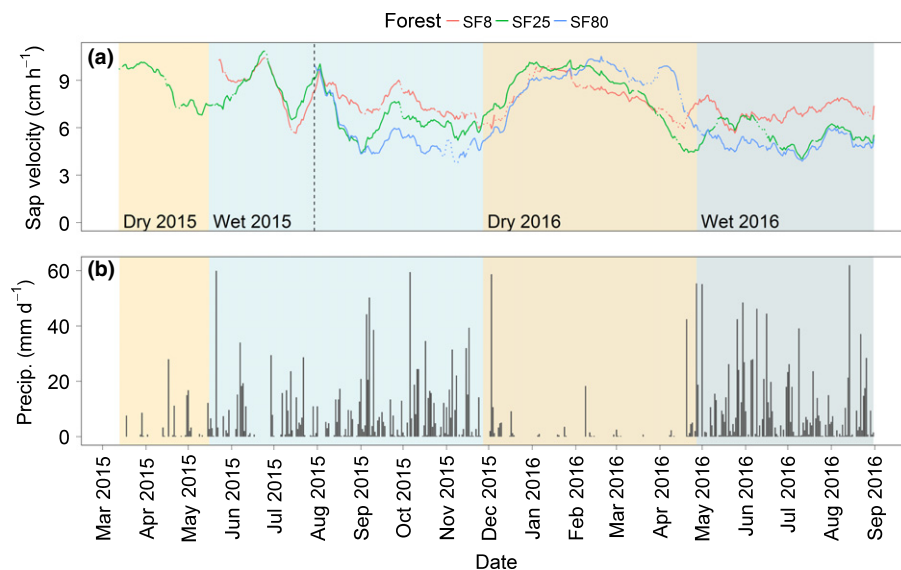
Fig. 4 Time series of 3-wk running mean (a) sap velocities (cm h^{-1}) and (b) precipitation (mm d^{-1}). Shaded areas denote seasons (tan, dry; blue, wet). The dashed line indicates the earliest date from which data across all forest ages are available (29 July 2015). Data from all trees are shown, with a minimum of 10 trees providing data per day out of 19, 28 and 27 trees in SF8, SF25 and SF80, respectively.

Discussion

Differences along the chronosequence

Our results show that tropical secondary forests in central Panama exhibited different seasonal behavior and response to drought-induced water limitations during the 2015–2016 ENSO event, with clear differences along the successional gradient. Amidst species-specific differences in hydraulic architecture, early-successional and light-demanding species are generally characterized by low wood densities and wide vessel diameters, resulting in higher hydraulic conductivity and transpiration rates that facilitate their typical fast growth behavior (Finegan, 1984; Granier *et al.*, 1996; Tyree *et al.*, 1998; Sack *et al.*, 2005; Poorter *et al.*, 2010). Forests in the AS project area reflect these patterns as they exhibit a shift of functional strategies from resource acquisition to resource conservation with progressing succession (Craven *et al.*, 2015). Although the observed differences in V_s and K_s between forest ages are nonsignificant and thus fail to support the first hypothesis – higher overall V_s and K_s as a result of higher water demands in early-successional forests – our data agree with the aforementioned general trends, as average V_s as well as K_s during the wet season decrease with progressing forest age (Fig. 5). The lack of significant differences in V_s between forests can be attributed in part to the similar wood densities of the instrumented trees in all forests, suggesting similar hydraulic architecture (Santiago *et al.*, 2004), as well as the strong seasonal, inversely phased fluctuations in V_s between forest ages (Fig. 4). The inclusion of additional trees from mature or primary forest in the chronosequence would further clarify whether the hypothesized trend is found along a broader successional gradient.

Our results partially lend support to the second hypothesis that water use was reduced in early-successional forest during the 2015–2016 ENSO dry season drought. Pronounced hysteresis loops, differences in Ψ_L and significant reductions in K_s during the dry season (Figs 2, 3a, 5) suggest stomatal regulation to prevent hydraulic failure in SF8 and SF25. Although K_s measurements are associated with uncertainties as a result of potential species-specific structural differences, K_s is not significantly related to wood density, thus further supporting environmental factors as drivers of the observed differences. Similar to our study, Huc *et al.* (1994) found that early-successional tropical rainforest species in French Guiana exhibit significantly decreased stomatal and plant-intrinsic hydraulic conductances and less negative midday Ψ_L, whereas late-successional species exhibit no change in the dry season. Although increasingly becoming the subject of debate (Hochberg *et al.*, 2017), isohydric behavior, that is, the maintenance of constant Ψ_L through the regulation of stomatal conductance, is a typical drought avoidance strategy (Bucci *et al.*, 2005), and has been shown to be a predominant trait in pioneer and early-successional species in a tropical dry forest in Bolivia (Markesteijn *et al.*, 2011). In central Panama, drought-intolerant species are associated with little tolerance to low leaf water status and relatively higher hydraulic stem conductances (Kursar *et al.*, 2009). Thus, although we did not directly assess drought tolerance by means of mortality or percentage loss of hydraulic conductivity, the greater response to soil VWC in SF8 (Fig. 7; Table 3) suggests that trees in early-successional forests experienced more drought stress than trees in late-successional forests, and consequently regulated water use during the 2015–16 ENSO dry season drought.

The third hypothesis, that late-successional forests did not limit water use during the 2015–2016 ENSO dry season drought, was supported by our data (Fig. 5a). Studies on seasonal differences of transpiration in tropical forests have reported inconsistent results, including higher whole-tree transpiration in the dry season (Meinzer *et al.*, 1999; O'Grady *et al.*, 1999; Schwendenmann *et al.*, 2015), similar canopy transpiration between
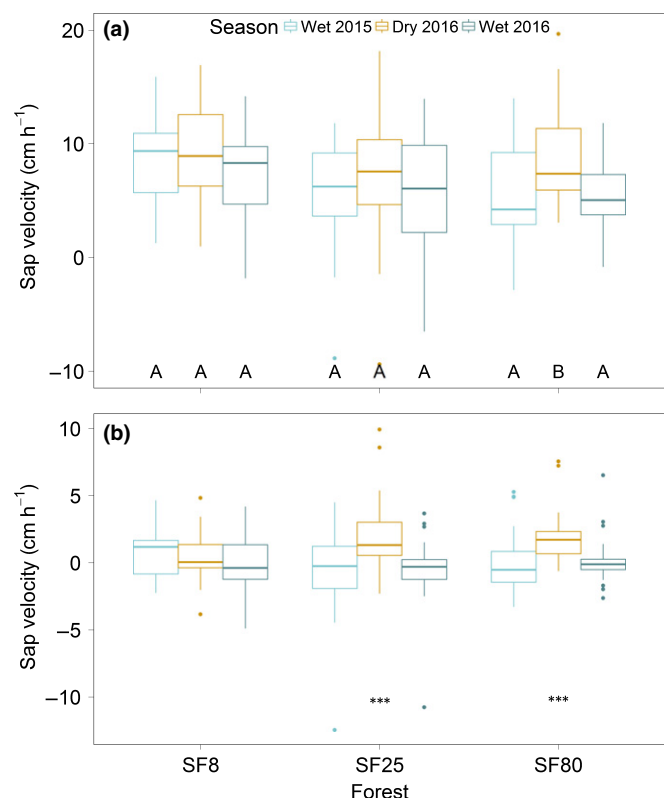
Fig. 5 Linear mixed model results of (a) diel and (b) nocturnal sap velocities in cm h^{-1} based on trees for which data were collected in all seasons ($N_{SF8} = 15$; $N_{SF25} = 25$; $N_{SF80} = 26$). Letters in (a) denote grouping, with different letters indicating significant differences in sap velocities between seasons within a given forest type ($\alpha < 0.05$; Tukey method). Asterisks (***) in (b) denote nocturnal sap velocities that were significantly different from 0. Data from 29 July 2015 to 31 August 2016. Horizontal lines inside boxes correspond to the median, the lower and upper box boundaries correspond to the first and third quartiles (25th and 75th percentiles, respectively), lower and upper whiskers extend no further than 1.5× inner quartile range (IQR) from the first and third quartiles, and dots represent data points beyond this range.

Fig. 6 Leaf water potential (Ψ_L, MPa) and corresponding sap flow (J, cm^3 m^{-2} s^{-1}) in SF8 (orange), SF25 (green) and SF80 (blue) in the (a) dry season and (b) wet season. J values were lagged up to 90 min, based on the highest correlation coefficient between (lagged) J and evaporative demand for a given tree on the day of measurement. Darcy's law approximations and respective standard error (SE) of sapwood-specific conductivity (K_s, mol m^{-2} s^{-1} MPa^{-1}) are given in the graphs.

seasons (Kumagai *et al.*, 2004) and higher stand transpiration in the wet season (McJannet *et al.*, 2007), suggesting complex interactions between taxonomic, physiognomic, microclimatic, edaphic and topographic factors. Canopy trees in Panama have been shown to exhibit little stomatal control, and CO$_2$ uptake is limited by light rather than water during the wet season (Phillips *et al.*, 2001; Graham *et al.*, 2003). In our study, V_s increased considerably in all forests at the beginning of the dry season when soils were still water saturated and cloud cover was low, lending support to light as the limiting factor of transpiration (Fig. 4). Several studies have found direct or indirect evidence that trees with access to deep soil water maintain a favorable plant water status and higher transpiration throughout periods of reduced moisture availability (Jackson *et al.*, 1995, 1999; Meinzer *et al.*, 1999; Stahl *et al.*, 2013; Schwendenmann *et al.*, 2015). In Panama, trees and lianas in old-growth forest utilize a higher proportion of deeper soil water at the end of the dry season (Andrade *et al.*, 2005). Although root architecture varies considerably by species in Panama, with some species allocating significantly
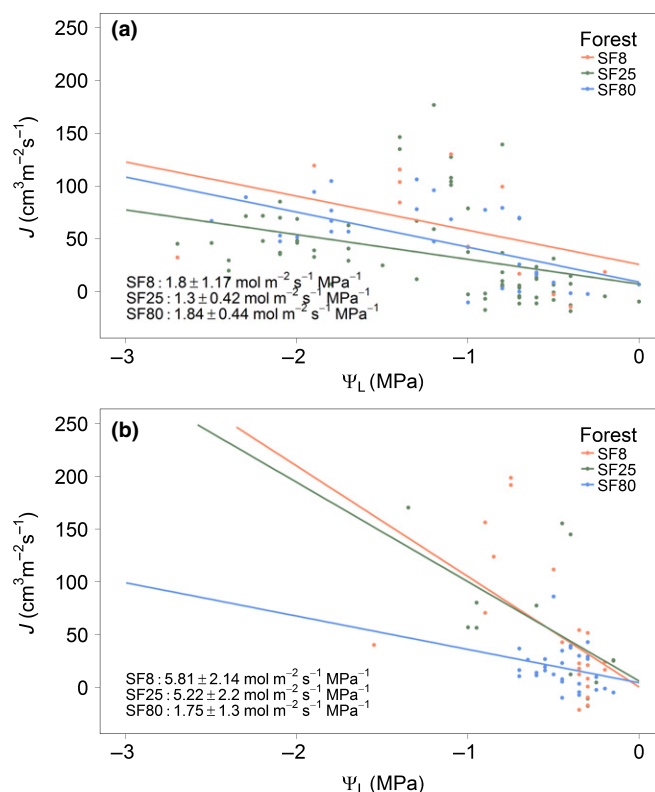
more resources to tap roots relative to lateral roots (Sinacore *et al.*, 2017), it can safely be assumed that long-established trees in SF80 have deeper, larger root systems relative to younger trees in SF8, providing one explanation for sustained higher V_s during the dry season in SF80. Despite clear evidence for differences in behavior with forest age during the 2015–2016 ENSO drought, long-term data are required to elucidate whether the observed differences between forests are a direct result of the drought or fall within the typical seasonal behavior.

Trees in Panama exhibit considerable stem water storage capacitance which is linearly related to sapwood area, with 10 kg of stored water per 0.1 m^2 of sapwood area (Goldstein *et al.*, 1998). The significant nocturnal sap flow observed in SF25 and SF80 during the dry season, when VPD was comparatively low, could be indicative of stem refilling in large trees with greater stem water capacitance (Forster, 2014). However, the benefits of stem water storage could be size independent, as stored stem water improved the tolerance to soil drought of only 1-yr-old late-successional species of a tropical dry forest in Mexico (Pineda-Garcia *et al.*, 2012, 2015), and had similar potential to alleviate hydraulic constraints in small and large trees in Panama (Phillips *et al.*, 2001). More research on whether stem capacitance has a disproportionally greater effect on drought avoidance in large trees relative to small trees is required, such as
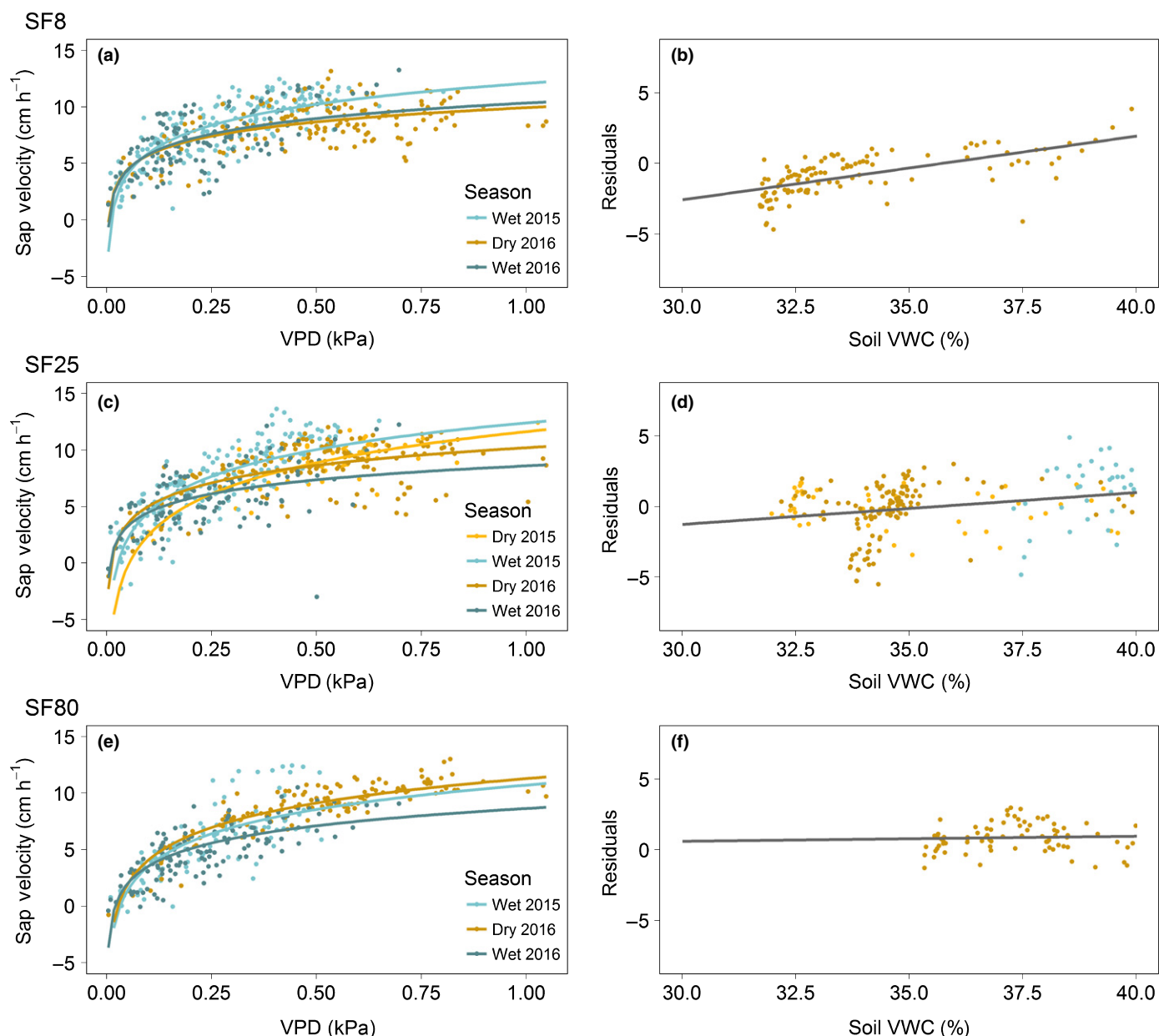
SF8

SF25

SF80

Fig. 7 (a, c, e) Linear regression of daily average vapor pressure deficit (VPD, kPa) and sap velocity (V_s, cm h^{-1}), and (b, d, f) residuals plotted against volumetric water content (%), in the top 50 cm of the soil in (a, b) SF8, (c, d) SF25 and (e, f) SF80. VPD explained (a) 48% (SF8), (c) 54% (SF25) and (e) 71% (SF80) of variance in V_s. Linear regression between residuals and soil volumetric water content (VWC) was significant in (b) SF8 ($R^2 = 0.42$, $P < 0.001$) and (d) SF25 ($R^2 = 0.7$, $P < 0.001$), and was nonsignificant in SF80 (f). Note how soil VWC does not go below 40% in the wet season in either (b) SF8 or (f) SF80. Single-variable regression of photosynthetic photon flux density (PPFD) and V_s explained 60%, 59% and 66% in SF8, SF25 and SF80, respectively, with similar relationships between residuals and VWC as above (Supporting Information Fig. S3).

simultaneous measurements of canopy conductance as well as sap flow at different heights in the stem and branches (Meinzer *et al.*, 2004), and in roots, across the chronosequence.

Environmental drivers

Our data lend support to the fourth hypothesis, that VPD replaces PPFD as the main driver of V_s in late-successional forests (Table 3). Light availability in the understory of secondary forest in Panama is reduced to < 10% of the above-canopy values after

20 yr of growth (van Breugel *et al.*, 2013). Consequently, the proportion of species with low light saturation points increases with progressing forest succession. As these species are adapted to low light conditions, VPD rather than PPFD becomes the primary limiting factor of transpiration in late-successional forests, making it one of the biological mechanisms that cause a feedback between microclimate and succession (Lebrija-Trejos *et al.*, 2011).

Taller canopies are generally more exposed to wind and thus better coupled to the atmosphere (Jarvis, 1984). In addition,

Table 3 Relative importance metrics and confidence intervals

Forest	Method	Predictor	Rel. imp. (%)	95% CI Upper	95% CI Lower
SF8	AVRG	PPFD	47.96	42.36	52.7
	AVRG	VPD	28.88	24.83	32.97
	AVRG	Precip.	10.99	6.78	15.58
	AVRG	VWC	8.09	5.44	11.5
	AVRG	WS	4.08	2.22	7.08
	LAST	PPFD	40.32	23.23	58.74
	LAST	VWC	31.42	18.68	42.47
	LAST	Precip.	15.49	8.07	23.85
	LAST	VPD	9.86	3.87	18.62
	LAST	WS	2.92	0.24	7.67
SF25	AVRG	PPFD	39.54	34.64	44.32
	AVRG	VPD	31.00	26.76	34.88
	AVRG	Precip.	12.59	8.91	17.09
	AVRG	WS	9.86	6.25	13.94
	AVRG	VWC	7.01	5.43	8.68
	LAST	PPFD	34.35	16.63	53.57
	LAST	Precip.	21.35	12.15	31.94
	LAST	VPD	20.72	9.84	33.39
	LAST	WS	12.24	4.26	22.43
	LAST	VWC	11.35	5.11	18.4
SF80	AVRG	VPD	35.23	31.64	38.66
	AVRG	PPFD	27.73	24.51	30.89
	AVRG	VWC	17.73	14.9	20.56
	AVRG	WS	13.01	9.61	16.66
	AVRG	Precip.	6.29	4.35	8.54
	LAST	VPD	55.75	38.2	69.12
	LAST	PPFD	18.06	7.31	31.13
	LAST	WS	12.59	4.52	23.08
	LAST	Precip.	9.87	4.53	17.03
	LAST	VWC	3.72	0.37	10.57

Methods are AVRG (overall model contribution averaged over orderings of predictors) and LAST (model contribution given all other predictors already included in the model). Data include all trees ($N_{SF8} = 19$, $N_{SF25} = 28$, $N_{SF80} = 27$). Predictors are photosynthetic photon flux density (PPFD), vapor pressure deficit (VPD), precipitation (Precip.), soil volumetric water content (VWC) and wind speed (WS). Note that predictors are sorted by relative importance for each metric and forest combination. Overall model performances were 69%, 66% and 86% for SF8, SF25 and SF80, respectively. A separate analysis of relative importance metrics on a subset of trees smaller than 15 cm in diameter at breast height (DBH) in SF25 and SF80 largely agrees with the results from the respective full models (Supporting Information Table S5).

transpiration in well-coupled canopies is mainly driven by VPD rather than radiation (Jarvis, 1984; Zhang *et al.*, 2014). The increasing relative importance of WS with progressing forest age, paired with the higher sensitivity of V_s to VPD, suggests a higher degree of canopy coupling in older forests as a result of increasing height. This is further supported by the smaller magnitude of the hysteresis between V_s and VPD in SF80 relative to SF8 and SF25, indicating that V_s is largely in phase with VPD in SF80. Estimates of omega decoupling coefficients (Jarvis, 1984) agree with this trend, with highest decoupling coefficients in SF8 and lowest decoupling coefficients in SF80 (Fig. S5).

The negative effect of precipitation on V_s is probably linked to leaf wetness, which had a strong inhibitory effect on sap flow in a tropical cloud forest tree in Brazil (Eller *et al.*, 2015) and reduced

transpiration by up to 28% in a tropical moist forest in central Costa Rica (Aparecido *et al.*, 2016). In the AS project area, canopy interception values approach levels of mature lowland forests after *c.* 10 yr of growth (Zimmermann *et al.*, 2013), explaining the observed significant difference in the effect of precipitation between SF8 and SF80. The counterclockwise hysteresis between PPFD and V_s in all forests, specifically the morning lag, could be indicative of either stem capacitance or the inhibition of diffusion as a result of leaf wetness from dew that accumulates on the leaves at night (O'Brien *et al.*, 2004).

The different effect of soil VWC on V_s between forests indicates that trees in SF8 and SF25 experience some degree of water limitation, whereas higher soil VWC has a negative effect on V_s in SF80. Soil VWC in SF80 remained comparatively wet throughout the dry season, never dropping below 35% (Figs 7f, 8). If soil VWC remains well above the threshold for trees to maintain a favorable plant water status, increases in soil VWC beyond that point will have no positive effect on V_s, but, instead, have the potential to reduce V_s as increases in VWC coincide with leaf wetting precipitation events. The difference in soil VWC during the dry season between forests (Fig. 8) could be indicative of a higher proportion of deep water usage of trees in SF80. Although not directly tested in this study, hydraulic redistribution by larger trees can relocate water from deep to more shallow soil layers, potentially facilitating the water access of understory trees (Dawson, 1996; Caldwell *et al.*, 1998; Oliveira *et al.*, 2005). The observed difference in soil VWC data during the dry season drought, paired with our sap flow data, indicates a feedback effect between soil properties and succession that has the potential to alleviate drought severity in older regrowing secondary forests in central Panama. Furthermore, soil water availability is a direct determinant of local and regional species distribution in tropical forest of Panama, and even short dry
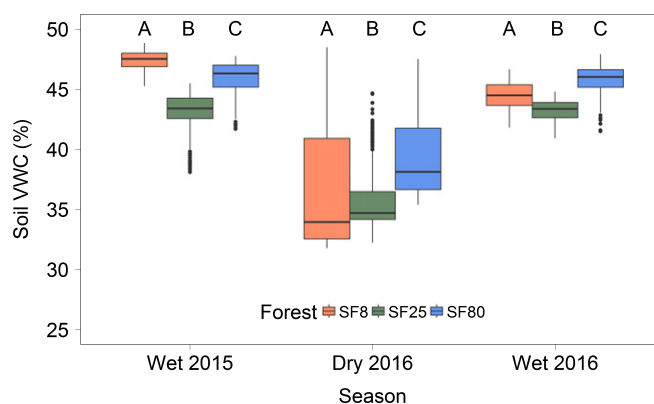

Fig. 8 Soil volumetric water content (%) in the top 50 cm of the soil in SF8 (orange), SF25 (green) and SF80 (blue). Data from 29 July 2015 to 31 August 2016. Horizontal lines inside boxes correspond to the median, the lower and upper box boundaries correspond to the first and third quartiles (25th and 75th percentiles, respectively), lower and upper whiskers extend no further than 1.5× inner quartile range (IQR) from the first and third quartiles, and dots represent data points beyond this range. Letters indicate significant differences in soil volumetric water content (VWC) between forests per season as assessed by linear mixed model and least square means pairwise comparison.

spells can cause significant mortality in establishing seedlings (Engelbrecht *et al.*, 2006, 2007). Water stress is a major factor in shaping geographic distributions of large trees in Panama (Meakem *et al.*, 2017). Contrary to SF8, both SF25 and SF80 have previously experienced droughts, including the severe 1997–1998 (SF25 and SF80) and 1982–1983 (SF80) ENSO events, potentially shifting species composition towards more drought-tolerant species in the older forests.

Conclusion

Our study shows that trees in early-successional forests displayed stronger signs of regulatory responses to the 2015–2016 ENSO drought, and that the limiting physiological processes for V_s shifted from operating at the plant–soil interface to the plant–atmosphere interface with progressing forest succession, probably as a result of favorable soil characteristics and access to deeper soil water in late-successional forests. A knowledge of the resilience of establishing secondary forests to drought is not only important for the optimization of reforestation efforts, but also for the development and optimization of models to predict water and carbon fluxes in a dynamic landscape that comprises a mosaic of pastures and forest fragments at different successional stages.

Author contributions

M.B., B.E.E. and J.S.H. designed the study. M.B. collected the data. M.B. carried out the data analysis with input from B.E.E. M.B. wrote the manuscript with revisions by all coauthors.

ORCID

Mario Bretfeld http://orcid.org/0000-0002-3875-9042

References

Allen RG, Pereira LS, Raes D, Smith M. 1998. *Crop evapotranspiration – guidelines for computing crop water requirements – FAO Irrigation and drainage paper 56*. Rome, Italy: FAO.

Andrade JL, Meinzer FC, Goldstein G, Schnitzer SA. 2005. Water uptake and transport in lianas and co-occurring trees of a seasonally dry tropical forest. *Trees* 19: 282–289.

Aparecido LMT, Miller GR, Cahill AT, Moore GW. 2016. Comparison of tree transpiration under wet and dry canopy conditions in a Costa Rican premontane tropical forest. *Hydrological Processes* 30: 5000–5011.

Apgaua DM, Ishida FY, Tng DY, Laidlaw MJ, Santos RM, Rumman R, Eamus D, Holtum JA, Laurance SG. 2015. Functional traits and water transport strategies in lowland tropical rainforest trees. *PLoS ONE* 10: e0130799.

Barrett D, Hatton T, Ash J, Ball M. 1995. Evaluation of the heat pulse velocity technique for measurement of sap flow in rainforest and eucalypt forest species of south-eastern Australia. *Plant, Cell & Environment* 18: 463–469.

Bates D, Mächler M, Bolker B, Walker S. 2015. Fitting linear mixed-effects models using lme4. *Journal of Statistical Software* 67: 1–48.

Bazzaz F, Pickett S. 1980. Physiological ecology of tropical succession: a comparative review. *Annual Review of Ecology and Systematics* 11: 287–310.

Bladon KD, Silins U, Landhäusser SM, Lieffers VJ. 2006. Differential transpiration by three boreal tree species in response to increased evaporative demand after variable retention harvesting. *Agricultural and Forest Meteorology* 138: 104–119.

Box GE, Cox DR. 1964. An analysis of transformations. *Journal of the Royal Statistical Society. Series B (Methodological)* 26: 211–252.

van Breugel M, Hall JS, Craven D, Bailon M, Hernandez A, Abbene M, van Breugel P. 2013. Succession of ephemeral secondary forests and their limited role for the conservation of floristic diversity in a human-modified tropical landscape. *PLoS ONE* 8: e82433.

Bucci SJ, Goldstein G, Meinzer FC, Franco AC, Campanello P, Scholz FG. 2005. Mechanisms contributing to seasonal homeostasis of minimum leaf water potential and predawn disequilibrium between soil and plant water potential in Neotropical savanna trees. *Trees* 19: 296–304.

Burgess SS, Adams MA, Turner NC, Beverly CR, Ong CK, Khan AA, Bleby TM. 2001. An improved heat pulse method to measure low and reverse rates of sap flow in woody plants. *Tree Physiology* 21: 589–598.

Caldwell MM, Dawson TE, Richards JH. 1998. Hydraulic lift: consequences of water efflux from the roots of plants. *Oecologia* 113: 151–161.

Čermák J, Kučera J, Bauerle WL, Phillips N, Hinckley TM. 2007. Tree water storage and its diurnal dynamics related to sap flow and changes in stem volume in old-growth Douglas-fir trees. *Tree Physiology* 27: 181–198.

Chevan A, Sutherland M. 1991. Hierarchical partitioning. *The American Statistician* 45: 90–96.

Craven D, Hall JS, Berlyn GP, Ashton MS, van Breugel M. 2015. Changing gears during succession: shifting functional strategies in young tropical secondary forests. *Oecologia* 179: 293–305.

Dawson TE. 1996. Determining water use by trees and forests from isotopic, energy balance and transpiration analyses: the roles of tree size and hydraulic lift. *Tree Physiology* 16: 263–272.

Eller CB, Burgess SS, Oliveira RS. 2015. Environmental controls in the water use patterns of a tropical cloud forest tree species, *Drimys brasiliensis* (Winteraceae). *Tree Physiology* 35: 387–399.

von Ende CN. 2001. Repeated-measures analysis: growth and other time-dependent measures. In: Scheiner SM, Gurevitch J, eds. *Design and analysis of ecological experiments*. New York, NY, USA: Oxford University Press, 134–157.

Engelbrecht BM, Comita LS, Condit R, Kursar TA, Tyree MT, Turner BL, Hubbell SP. 2007. Drought sensitivity shapes species distribution patterns in tropical forests. *Nature* 447: 80–82.

Engelbrecht BM, Dalling JW, Pearson TR, Wolf RL, Galvez DA, Koehler T, Tyree MT, Kursar TA. 2006. Short dry spells in the wet season increase mortality of tropical pioneer seedlings. *Oecologia* 148: 258–269.

Escudero A, Valladares F. 2016. Trait-based plant ecology: moving towards a unifying species coexistence theory. *Oecologia* 180: 919–922.

Ewers BE, Bond-Lamberty B, Mackay DS. 2011. Consequences of stand age and species' functional trait changes on ecosystem water use of forests. In: Meinzer FC, Lachenbruch B, Dawson TE, eds. *Size- and age-related changes in tree structure and function*. Netherlands: Springer, 481–505.

Finegan B. 1984. Forest succession. *Nature* 312: 109–114.

Forster MA. 2014. How significant is nocturnal sap flow? *Tree Physiology* 34: 757–765.

Goldstein G, Andrade J, Meinzer F, Holbrook N, Cavelier J, Jackson P, Celis A. 1998. Stem water storage and diurnal patterns of water use in tropical forest canopy trees. *Plant, Cell & Environment* 21: 397–406.

Graham EA, Mulkey SS, Kitajima K, Phillips NG, Wright SJ. 2003. Cloud cover limits net CO$_2$ uptake and growth of a rainforest tree during tropical rainy seasons. *Proceedings of the National Academy of Sciences, USA* 100: 572–576.

Granier A, Huc R, Barigah S. 1996. Transpiration of natural rain forest and its dependence on climatic factors. *Agricultural and Forest Meteorology* 78: 19–29.

Grömping U. 2006. Relative importance for linear regression in R: the package relaimpo. *Journal of Statistical Software* 17: 1–27.

Hadfield JD. 2010. MCMC methods for multi-response generalized linear mixed models: the MCMCglmm R package. *Journal of Statistical Software* 33: 1–22.

Hansen J, Sato M. 2016. Regional climate change and national responsibilities. *Environmental Research Letters* 11: 034009.

Hernandez-Santana V, Hernandez-Hernandez A, Vadeboncoeur MA, Asbjornsen H. 2015. Scaling from single-point sap velocity measurements to stand transpiration in a multispecies deciduous forest: uncertainty sources, stand structure effect, and future scenarios. *Canadian Journal of Forest Research* 45: 1489–1497.

Hochberg U, Rockwell FE, Holbrook NM, Cochard H. 2017. Iso/Anisohydry: a plant–environment interaction rather than a simple hydraulic trait. *Trends in Plant Science* 23: 112–120.

Hothorn T, Bretz F, Westfall P. 2008. Simultaneous inference in general parametric models. *Biometrical Journal* 50: 346–363.

Huc R, Ferhi A, Guehl J. 1994. Pioneer and late stage tropical rainforest tree species (French Guiana) growing under common conditions differ in leaf gas exchange regulation, carbon isotope discrimination and leaf water potential. *Oecologia* 99: 297–305.

Jackson P, Cavelier J, Goldstein G, Meinzer F, Holbrook N. 1995. Partitioning of water resources among plants of a lowland tropical forest. *Oecologia* 101: 197–203.

Jackson PC, Meinzer FC, Bustamante M, Goldstein G, Franco A, Rundel PW, Caldas L, Igler E, Causin F. 1999. Partitioning of soil water among tree species in a Brazilian Cerrado ecosystem. *Tree Physiology* 19: 717–724.

Jarvis P. 1984. Coupling of transpiration to the atmosphere in horticultural crops: the omega factor. *I International Symposium on Water Relations in Fruit Crops* 171: 187–206.

Johnson EA, Miyanishi K. 2008. Testing the assumptions of chronosequences in succession. *Ecology Letters* 11: 419–431.

Komatsu H, Kume T, Shinohara Y. 2017. Optimal sap flux sensor allocation for stand transpiration estimates: a non-dimensional analysis. *Annals of Forest Science* 74: 38.

Kumagai T'o, Saitoh TM, Sato Y, Morooka T, Manfroi OJ, Kuraji K, Suzuki M. 2004. Transpiration, canopy conductance and the decoupling coefficient of a lowland mixed dipterocarp forest in Sarawak, Borneo: dry spell effects. *Journal of Hydrology* 287: 237–251.

Kunert N, Schwendenmann L, Hölscher D. 2010. Seasonal dynamics of tree sap flux and water use in nine species in Panamanian forest plantations. *Agricultural and Forest Meteorology* 150: 411–419.

Kursar TA, Engelbrecht BM, Burke A, Tyree MT, El Omari B, Giraldo JP. 2009. Tolerance to low leaf water status of tropical tree seedlings is related to drought performance and distribution. *Functional Ecology* 23: 93–102.

Lebrija-Trejos E, Pérez-García EA, Meave JA, Poorter L, Bongers F. 2011. Environmental changes during secondary succession in a tropical dry forest in Mexico. *Journal of Tropical Ecology* 27: 477–489.

Luo Z, Guan H, Zhang X, Zhang C, Liu N, Li G. 2016. Responses of plant water use to a severe summer drought for two subtropical tree species in the central southern China. *Journal of Hydrology: Regional Studies* 8: 1–9.

Mallick K, Trebs I, Boegh E, Giustarini L, Schlerf M, Drewry DT, Hoffmann L, Randow Cv, Kruijt B, Araùjo A. 2016. Canopy-scale biophysical controls of transpiration and evaporation in the Amazon Basin. *Hydrology and Earth System Sciences* 20: 4237–4264.

Markesteijn L, Poorter L, Bongers F, Paz H, Sack L. 2011. Hydraulics and life history of tropical dry forest tree species: coordination of species' drought and shade tolerance. *New Phytologist* 191: 480–495.

Marshall D. 1958. Measurement of sap flow in conifers by heat transport. *Plant Physiology* 33: 385.

Martínez-Vilalta J, Poyatos R, Aguadé D, Retana J, Mencuccini M. 2014. A new look at water transport regulation in plants. *New Phytologist* 204: 105–115.

Matheny AM, Bohrer G, Vogel CS, Morin TH, He L, Frasson RPdM, Mirfenderesgi G, Schäfer KV, Gough CM, Ivanov VY. 2014. Species-specific transpiration responses to intermediate disturbance in a northern hardwood forest. *Journal of Geophysical Research: Biogeosciences* 119: 2292–2311.

McGill BJ, Enquist BJ, Weiher E, Westoby M. 2006. Rebuilding community ecology from functional traits. *Trends in Ecology & Evolution* 21: 178–185.

McJannet D, Fitch P, Disher M, Wallace J. 2007. Measurements of transpiration in four tropical rainforest types of north Queensland, Australia. *Hydrological Processes* 21: 3549–3564.

Meakem V, Tepley AJ, Gonzalez-Akre EB, Herrmann V, Muller-Landau HC, Wright SJ, Hubbell SP, Condit R, Anderson-Teixeira KJ. 2017. Role of tree size in moist tropical forest carbon cycling and water deficit responses. *New Phytologist*. doi: 10.1111/nph.14633.

Meinzer FC, Andrade JL, Goldstein G, Holbrook NM, Cavelier J, Wright SJ. 1999. Partitioning of soil water among canopy trees in a seasonally dry tropical forest. *Oecologia* 121: 293–301.

Meinzer F, Goldstein G, Andrade J. 2001. Regulation of water flux through tropical forest canopy trees: do universal rules apply? *Tree Physiology* 21: 19–26.

Meinzer FC, James SA, Goldstein G. 2004. Dynamics of transpiration, sap flow and use of stored water in tropical forest canopy trees. *Tree Physiology* 24: 901–909.

Monteith JL. 1965. Evaporation and environment. In: *The state and movement of water in living organisms, Proc. 19th Symp*. Swansea, UK: Society of Experimental Biology. Cambridge University Press, 205–234.

Moore GW, Orozco G, Aparecido LM, Miller GR. 2017. Upscaling transpiration in diverse forests: insights from a tropical premontane site. *Ecohydrology*. doi: 10.1002/eco.1920

Nepstad DC, Tohver IM, Ray D, Moutinho P, Cardinot G. 2007. Mortality of large trees and lianas following experimental drought in an Amazon forest. *Ecology* 88: 2259–2269.

Norden N, Angarita HA, Bongers F, Martínez-Ramos M, Granzow-de la Cerda I, Van Breugel M, Lebrija-Trejos E, Meave JA, Vandermeer J, Williamson GB. 2015. Successional dynamics in Neotropical forests are as uncertain as they are predictable. *Proceedings of the National Academy of Sciences, USA* 112: 8013–8018.

Oberbauer SF, Strain BR, Riechers G. 1987. Field water relations of a wet-tropical forest tree species, *Pentaclethra macroloba* (Mimosaceae). *Oecologia* 71: 369–374.

O'Brien JJ, Oberbauer SF, Clark DB. 2004. Whole tree xylem sap flow responses to multiple environmental variables in a wet tropical forest. *Plant, Cell & Environment* 27: 551–567.

Ogden FL, Crouch TD, Stallard RF, Hall JS. 2013. Effect of land cover and use on dry season river runoff, runoff efficiency, and peak storm runoff in the seasonal tropics of Central Panama. *Water Resources Research* 49: 8443–8462.

O'Grady A, Eamus D, Hutley L. 1999. Transpiration increases during the dry season: patterns of tree water use in eucalypt open-forests of northern Australia. *Tree Physiology* 19: 591–597.

Oliveira RS, Dawson TE, Burgess SS, Nepstad DC. 2005. Hydraulic redistribution in three Amazonian trees. *Oecologia* 145: 354–363.

Oren R, Ewers BE, Todd P, Phillips N, Katul G. 1998. Water balance delineates the soil layer in which moisture affects canopy conductance. *Ecological Applications* 8: 990–1002.

Oren R, Phillips N, Ewers B, Pataki D, Megonigal J. 1999. Sap-flux-scaled transpiration responses to light, vapor pressure deficit, and leaf area reduction in a flooded *Taxodium distichum* forest. *Tree Physiology* 19: 337–347.

Penman HL. 1948. Natural evaporation from open water, bare soil and grass. *Proceedings of the Royal Society of London A: Mathematical, Physical and Engineering Sciences* 193: 120–145.

Pfautsch S, Adams MA. 2013. Water flux of *Eucalyptus regnans*: defying summer drought and a record heatwave in 2009. *Oecologia* 172: 317–326.

Phillips N, Bond BJ, Ryan MG. 2001. Gas exchange and hydraulic properties in the crowns of two tree species in a Panamanian moist forest. *Trees–Structure and Function* 15: 123–130.

Phillips N, Oren R, Zimmermann R, Wright SJ. 1999. Temporal patterns of water flux in trees and lianas in a Panamanian moist forest. *Trees–Structure and Function* 14: 116–123.

Phillips N, Ryan M, Bond B, McDowell N, Hinckley T, Čermák J. 2003. Reliance on stored water increases with tree size in three species in the Pacific Northwest. *Tree Physiology* 23: 237–245.

Phillips OL, Aragão LEOC, Lewis SL, Fisher JB, Lloyd J, López-González G, Malhi Y, Monteagudo A, Peacock J, Quesada CA *et al.* 2009. Drought sensitivity of the Amazon rainforest. *Science* 323: 1344–1347.

Pineda-Garcia F, Paz H, Meinzer FC. 2012. Drought resistance in early and late secondary successional species from a tropical dry forest: the interplay between xylem resistance to embolism, sapwood water storage and leaf shedding. *Plant, Cell & Environment* 36: 405–418.

Pineda-Garcia F, Paz H, Meinzer FC, Angeles G. 2015. Exploiting water versus tolerating drought: water-use strategies of trees in a secondary successional tropical dry forest. *Tree Physiology* 36: 208–217.

Poorter L, McDonald I, Alarcón A, Fichtler E, Licona JC, Peña-Claros M, Sterck F, Villegas Z, Sass-Klaassen U. 2010. The importance of wood traits and hydraulic conductance for the performance and life history strategies of 42 rainforest tree species. *New Phytologist* 185: 481–492.

Poorter L, van de Plassche M, Willems S, Boot RGA. 2004. Leaf traits and herbivory rates of tropical tree species differing in successional status. *Plant Biology* 6: 746–754.

Powell TL, Galbraith DR, Christoffersen BO, Harper A, Imbuzeiro H, Rowland L, Almeida S, Brando PM, Costa ACL, Costa MH. 2013. Confronting model predictions of carbon fluxes with measurements of Amazon forests subjected to experimental drought. *New Phytologist* 200: 350–365.

Powell TL, Wheeler JK, de Oliveira AA, da Costa L, Carlos A, Saleska SR, Meir P, Moorcroft PR. 2017. Differences in xylem and leaf hydraulic traits explain differences in drought tolerance among mature Amazon rainforest trees. *Global Change Biology* 23: 4280–4293.

R Core Team 2015. *R: a language and environment for statistical computing (version 3.3.2).* Vienna, Austria: R Foundation for Statistical Computing.

Rowland L, Da Costa A, Galbraith D, Oliveira R, Binks O, Oliveira A, Pullen A, Doughty C, Metcalfe D, Vasconcelos S. 2015. Death from drought in tropical forests is triggered by hydraulics not carbon starvation. *Nature* 528: 119–122.

Sack L, Tyree MT, Holbrook NM. 2005. Leaf hydraulic architecture correlates with regeneration irradiance in tropical rainforest trees. *New Phytologist* 167: 403–413.

Santiago L, Goldstein G, Meinzer F, Fisher J, Machado K, Woodruff D, Jones T. 2004. Leaf photosynthetic traits scale with hydraulic conductivity and wood density in Panamanian forest canopy trees. *Oecologia* 140: 543–550.

Schönbeck L, Lohbeck M, Bongers F, Ramos M, Sterck F. 2015. How do light and water acquisition strategies affect species selection during secondary succession in moist tropical forests? *Forests* 6: 2047.

Schwendenmann L, Pendall E, Sanchez-Bragado R, Kunert N, Hölscher D. 2015. Tree water uptake in a tropical plantation varying in tree diversity: interspecific differences, seasonal shifts and complementarity. *Ecohydrology* 8: 1–12.

Sinacore K, Hall JS, Potvin C, Royo AA, Ducey MJ, Ashton MS. 2017. Unearthing the hidden world of roots: root biomass and architecture differ among species within the same guild. *PLoS ONE* 12: e0185934.

Stahl C, Burban B, Wagner F, Goret JY, Bompy F, Bonal D. 2013. Influence of seasonal variations in soil water availability on gas exchange of tropical canopy trees. *Biotropica* 45: 155–164.

Turner BL, Engelbrecht BM. 2011. Soil organic phosphorus in lowland tropical rain forests. *Biogeochemistry* 103: 297–315.

Tyree MT, Engelbrecht BM, Vargas G, Kursar TA. 2003. Desiccation tolerance of five tropical seedlings in Panama. Relationship to a field assessment of drought performance. *Plant Physiology* 132: 1439–1447.

Tyree MT, Ewers FW. 1991. The hydraulic architecture of trees and other woody plants. *New Phytologist* 119: 345–360.

Tyree MT, Sperry JS. 1989. Vulnerability of xylem to cavitation and embolism. *Annual Review of Plant Biology* 40: 19–36.

Tyree MT, Velez V, Dalling J. 1998. Growth dynamics of root and shoot hydraulic conductance in seedlings of five neotropical tree species: scaling to show possible adaptation to differing light regimes. *Oecologia* 114: 293–298.

Van Bavel C. 1966. Potential evaporation: the combination concept and its experimental verification. *Water Resources Research* 2: 455–467.

Wolfe BT, Sperry JS, Kursar TA. 2016. Does leaf shedding protect stems from cavitation during seasonal droughts? A test of the hydraulic fuse hypothesis. *New Phytologist* 212: 1007–1018.

Wright SJ. 2010. The future of tropical forests. *Annals of the New York Academy of Sciences* 1195: 1–27.

Wright SJ, Kitajima K, Kraft NJ, Reich PB, Wright IJ, Bunker DE, Condit R, Dalling JW, Davies SJ, Díaz S. 2010. Functional traits and the growth–mortality trade-off in tropical trees. *Ecology* 91: 3664–3674.

Zhang Q, Manzoni S, Katul G, Porporato A, Yang D. 2014. The hysteretic evapotranspiration–vapor pressure deficit relation. *Journal of Geophysical Research: Biogeosciences* 119: 125–140.

Zimmermann B, Zimmermann A, Scheckenbach H, Schmid T, Hall J, van Breugel M. 2013. Changes in rainfall interception along a secondary forest succession gradient in lowland Panama. *Hydrology and Earth System Sciences* 17: 4659–4670.

Supporting Information

Additional Supporting Information may be found online in the Supporting Information tab for this article:

Fig. S1 Boxplots of leaf water potentials at different canopy positions from eight species ($n = 36$) in SF80.

Fig. S2 Minimum number of working sap flow sensors and resulting standard deviation (SD) of average sap velocity data for all forests.

Fig. S3 Linear regression of daily average photosynthetic photon flux density (PPFD) ($\mu mol\,m^{-2}\,s^{-1}$) and sap velocity V_s ($cm\,h^{-1}$), and model residuals plotted against volumetric water content (%) in the top 50 cm of the soil.

Fig. S4 Time series of 3-wk running mean sap velocities and sum of daily precipitation, excluding four *Annona spraguei* and one *Casearia arborea* in SF25 because of their long-term dormancy at the end of the 2016 dry season.

Fig. S5 Boxplot of average daily omega decoupling coefficients for all forests and seasons.

Table S1 Overview of sap flow site characteristics, including GPS coordinates, slope, aspect, slope length and elevation

Table S2 Overview of instrumented species and their phenology, relative canopy position, diameter at breast height (cm) and wood density ($g\,cm^{-3}$)

Table S3 Overview of instrumented species, respective sampling periods and number of days in which no data were collected (e.g. as a result of equipment failure)

Table S4 ANOVA table of generalized linear mixed model results (M-2) and parameter estimates and *P* values based on the Markov Chain Monte Carlo method with 1000 iterations

Table S5 Relative importance metrics and confidence intervals of trees of < 15 cm diameter at breast height (DBH) (NSF8 = 19; NSF25 = 11; NSF80 = 13)

Table S6 Relative importance metrics and confidence intervals for SF25, excluding four *Annona spraguei* and one *Casearia arborea* because of their long-term dormancy at the end of the dry season

Please note: Wiley Blackwell are not responsible for the content or functionality of any Supporting Information supplied by the authors. Any queries (other than missing material) should be directed to the *New Phytologist* Central Office.

About *New Phytologist*

- *New Phytologist* is an electronic (online-only) journal owned by the New Phytologist Trust, a **not-for-profit organization** dedicated to the promotion of plant science, facilitating projects from symposia to free access for our Tansley reviews and Tansley insights.

- Regular papers, Letters, Research reviews, Rapid reports and both Modelling/Theory and Methods papers are encouraged. We are committed to rapid processing, from online submission through to publication 'as ready' via *Early View* – our average time to decision is <26 days. There are **no page or colour charges** and a PDF version will be provided for each article.

- The journal is available online at Wiley Online Library. Visit **www.newphytologist.com** to search the articles and register for table of contents email alerts.

- If you have any questions, do get in touch with Central Office (np-centraloffice@lancaster.ac.uk) or, if it is more convenient, our USA Office (np-usaoffice@lancaster.ac.uk)

- For submission instructions, subscription and all the latest information visit **www.newphytologist.com**